

Ground-based light curve follow-up validation observations of TESS object of interest TOI 3779.01

Samuel T. Joseph¹, Dr. Peter P. Plavchan²

1. Evergreen Valley High School, San Jose, CA

2. Department of Physics and Astronomy, 4400 University Drive MS 3F3, George Mason University, Fairfax, VA 22030, USA

Abstract

The objective of this study is to determine if TESS object of interest TOI 3779.01 is an exoplanet which is currently classified as a possible candidate in the NASA Exoplanet Archive. The raw telescope data of TOI 3779.01 was collected from the GMU Observatory. These images were reduced, plate solved, and aligned using AstroImageJ to generate a light curve of TOI 3779.01's transit. There is a dimming of the host star during the transit period, however, since there was notable light pollution during the observational night and nearby reference stars failed the NEB (Nearby Eclipsing Binary) check, the aperture could have been contaminated. To find the planet-to-star radius ratio of TOI 3779.01 we first used the transit depth (6.93 ppt) calculated from our transit model in AstroImageJ to get a ratio value of 0.083246. Using the transit model ratio and transit depth, the radius of TOI 3779.01 is 0.09152 R_{\odot} (stellar radius). This value comes close with two other estimates: the first is using the TESS predicted transit depth (8.8) which yielded 0.103189 R_{\odot} and the other is a python probabilistic model which predicted 0.037. These calculations assumes that the stellar radius of the host star is 1.1 R_{\odot} . Based on the large radius, we classified TOI 3779.01 as a Hot Jupiter. However, since the aperture was contaminated, the findings of this study can be further used by the TESS team to do more research employing other methods like spectroscopy and chromaticity.

1. Introduction

Any planet not present in our solar system is classified as an Exoplanet with over 5500 confirmed and 9800 possible exoplanet candidates discovered by the NASA missions including TESS- Transiting Exoplanet Survey Satellite (1). TESS is a telescope designed by NASA launched in 2018 on the SpaceX Falcon 9 (2). It divides the sky into 26 sectors, each observable for 27.4 days and employs the transit method, which is by far the most successful in detecting small exoplanets (2). In the transit method the exoplanets must pass in front of its star from our perspective on ground, dimming the light from the star (2). The detection of dimming of the host star due to the transit is a good indication the planet is an exoplanet but it does not fully confirm that it is an exoplanet. If there is more than one detection of a transit in the TESS data the planet is considered a possible candidate (Conti, 2020). From here based on different cases, the exoplanet can be classified into many different categories outlined in the TFOP guidelines.

The search for exoplanets has become a larger study overtime in astronomy especially now and this is largely to find extraterrestrial life outside earth (1). The purpose of this paper is to help the TESS team confirm if TOI 3779.01 is an exoplanet by using modeling techniques. Ground-based observations of

exoplanets is not something new but has been done by many other researchers and they all have the same goal of characterizing and classifying their exoplanets. *Another Shipment of Six Short-Period Giant Planets from TESS* written by Joseph E. Rodriguez et al was focussed on characterizing 6 different giant exoplanets. They were able to determine that their planets were Jovian-sized planets along with their masses, periods, and the type of host stars the planets orbits (Rodriguez, 2023). While this research focused on giant exoplanets, *Ground-based Follow-up Observations of TESS Exoplanet Candidates* written by Sarah Tang and William Waalkes was aimed to classify the type of exoplanet LHS 3844 b and similar other candidates were. They used AstroImageJ and python to process the image data into flux light curves. (Tang, 2020). Using the fitted light curve model they generated, they classified LHS 3844 b to be a terrestrial planet. Our research is really similar to what Tang did with her ground-based follow-up observation, however, the focus of our research is TOI 3779.01 which is classified as a possible candidate. We will use python and AstroImageJ to model light curves of the transit to classify the type of exoplanet.

In this paper, we present follow-up observations of TOI 3779.01. The raw images were collected on a

32" Ritchey-Chretien Telescope with a SBIG 16803 visible CCD from the GMU observatory. The predicted ingress times and egress times of the transit are 0:01 and 1:00 with an orbital period of 1.618 days and predicted transit depth of 17254.798 ppm (6). Based on the predicted ingress and egress times we will be investigating if a transit will occur in that time period with a transit depth close to the predicted transit depth. Most of the public exoplanet databases of TOI 3779.01 have limited data on its planetary and

2. Observations

The TESS Team data in *Table 1* (7) are predictions of TOI 3779.01's transit on the day we collected the data. The predicted orbital period of TOI 3779.01 is 1.618 days which has a full transit time of about an hour (7). However, we collected 10 hours of data both before and after the transit giving us enough data to model a light curve.

There was considerable light pollution on the day of data collection which could have caused contamination to the aperture. According to the TESS team the blending companion is only 0.779" (7), making our perspective on the ground look blended. The light from nearby stars blends with the light of the host star interfering with the transit. While this could entail that TOI 3779.01 is a false positive, we will do more investigation and tests to classify it.

stellar parameters. One of the goals of this paper is to determine the planet radius $[R_{\text{Earth}}]$ of the TOI 3779.01.

In section 2, we present our observations prior to the analysis of our data. In section 3, we present our analysis and methods of modeling our light curves. In section 4, we present our finalized results. In section 5, we discuss our results. In section 6, we present our conclusions and future work.

	Data	Source
Date Recorded	Mon. 2023-02-13	GMU Observatory
Start Time - End Time	18:45 - 4:40	GMU Observatory
Exposure Time	95s	GMU Observatory
Filter	R	GMU Observatory
Right Ascension [sexagesimal] (RA), Declination [sexagesimal] (DEC)	06h58m55.97s, +49d58m07.45s	NASA Archive (6)
Ingress, Egress	0:01, 1:00 $\pm 0:03$	TESS Team (7)
Type of Transit	Full Transit	TESS Team (7)
Duration of Transit	$0:59 \pm 0:14$	TESS Team (7)
Orbital Period	1.618 days	NASA Archive (6)

Table 1 Preliminary Data on TOI 3779.01

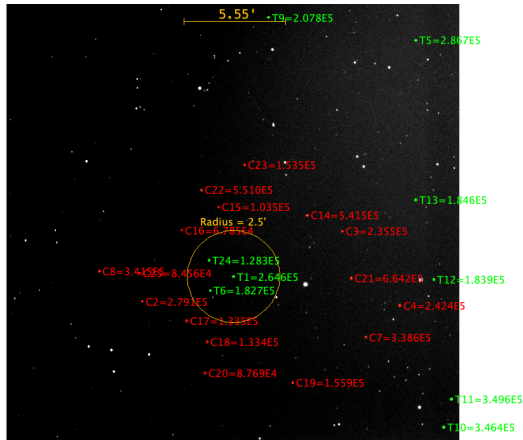


Figure 1 Field Image. T1 is the target star and the red stars are the reference stars.

3. Analysis

In section 3.1 we present the tools needed for light curve and probabilistic modeling. In section 3.2 we discuss the process of data reduction. In section 3.3 we discuss how to plate solve and align images. In section 3.4 we present how to perform aperture photometry to generate a measurement table that is used for modeling a light curve. In section 3.5 we present how to perform a NEB analysis. In section 3.6 we present the process of modeling a light curve. In section 3.7 we discuss the process of probabilistic transit modeling. The analysis in this paper is shortened; nevertheless, more comprehensive guided instructions are available in the Campus Telescope TESS Follow-Up Light Curve Tutorial by Plavchan et al. (8) and exoplanet by Mackey (9).

3.1 Tool kit to analyze

The only tool needed for light curve modeling is AstroImageJ which is a powerful image analysis software used to generate light curves and analysis of an exoplanet transit (10). To perform probabilistic modeling we used the *exoplanet* python package (Mackey, 2018). This package is really similar to the more commonly known *batman* python package used for modeling exoplanet transits (11). However, *exoplanet* is built on an Aesara/Theano operation that uses bayesian analysis and other packages like PyMC3 and numpy to create complex models.

3.2 Data Reduction

The images we collected from the GMU Observatory were 10 dark, 10 flat, and 167 science images stored as .fits files. These images were taken with an exposure time of 95s and filter R. To process these images to generate a light curve we first reduced these images. Data reduction is necessary to remove any noise and background artifacts in the science

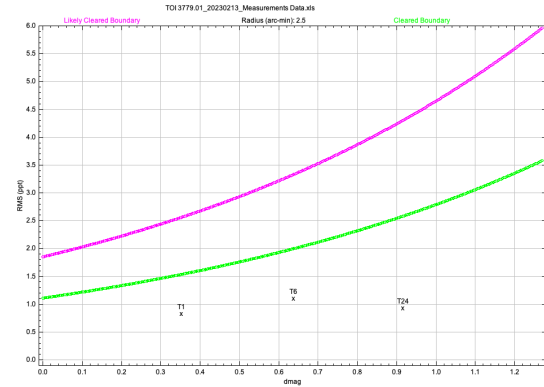


Figure 2 NEB Analysis Plot. The target star (T1) and the reference stars (T6 and T24) did not clear the NEB check.

images. The dark images were taken with the shutter of the camera closed to get rid of any thermal noise that stemmed from the CCD sensor. While the flat images were taken with the shutter completely opened to get rid of any artificial noise by correcting any defective pixels and vignetting. We also remove any science images that had unusual artifacts caused by external sources like a satellite or plane passing by during the collection of the image. Using the DP coordinate Converter and CCD Data processor in AstroImageJ we subtracted the dark and the flat images to create a master subtracted dark and flat image. The science images were also data reduced before plate solving.

3.3 Plate Solving and Aligning Images

Plate solving is a process that assigns every object in a frame with a corresponding RA (right ascension) and DEC (declination) coordinates. This is a crucial step as it identifies and differentiates the target host star from the reference stars around it when light curve modeling and doing analysis. To plate solve our reduced images we first enter the user key acquired from nova.astrometry.net and edit the parameters of our target in the “DP Astrometry Settings” of AstroImageJ. To precisely track the time we switched BJD_UTC to BJD_TBD in the “General FITS Header Settings” of AstroImageJ before plate solving our reduced images. The plate solved images are saved in a new subdirectory named “pipelineout”. If the reduced images are not plate solved, the images must be aligned before generating a light curve. We removed any images that had large movements and jumps before the aligning process. Using the “Stack Aligner” in AstroImageJ we set a radius of the target object aperture, the inner radius of the background annulus, and the outer radius of the background annulus. With those parameters we placed an aperture

on our target star and also on a few reference stars for aligning the images. The aligned images were then saved in a subdirectory named “Aligned”. The images are now fully processed including data reduction, plate solving, and alignment, in preparation for creating a measuring table for our light curve.

3.4 Aperture Photometry and Measurement Table

To generate a measurement table that is used to plot a light curve we need to first perform aperture photometry. Aperture photometry is the process of measuring the light in an aperture which is a circular region with a set radius in an image (12). When selecting apertures for the target host star and reference stars they must be of the right size only capturing the light of the selected star. To find the right size of the aperture we need of our target host star we used the “Aperture Photometry Tool” in AstroImageJ to select our target star which can be identified using an annotated finder chart from Astronomy at Swarthmore College (13). A “Seeing Profile” will be generated with a radius, background’s inner, and outer radii which can be used to set the size of the aperture. However, the aperture sizes in our seeing profile were too wide so we chose our own aperture sizes. The base radius of object aperture we used was 10, the inner radius of background annulus was 17, and the outer radius of background annulus was 25. We annotated our field image by adding a 2.5 inch radius circle around the target star which will be helpful for performing multi-aperture photometry.

Using the “Multi-Aperture Measurement” feature we set the aperture parameters to the same radius values we chose for our target host star aperture. We placed the green T1 aperture on our target star and the rest of the red apertures starting with C1 on our reference stars. The reference stars chosen are similar in size and brightness to the target star T1 (*Figure 1*). After selecting all our reference stars, AstroImageJ generates a measurement table with all the data needed to plot our light curve.

3.5 NEB Analysis

In section 3.4 we chose the target host star and 24 other reference stars to perform multi-aperture photometry. Of all the chosen reference stars only 2 of them were present in the 2.5 inch radius circular region from the target host star. These two reference stars can contaminate the aperture and light coming from T1 so we used the “TFOP SG1 NEB Analysis Macro” tool in AstroImageJ to test if T1 is a NEB (Nearby Eclipsing Binary). A nearby eclipsing binary

is a binary star system where both stars orbit their center of gravity (14). On earth an NEB would be visible as one star so when one of the stars passes in front of the other in the system the light flux would drop on the NEB’s light curve (14). An NEB can not be classified as an exoplanet because in an exoplanet transit a planet must pass in front of the host star, not another star. This check will generate plots that can be used to see if T1 is an NEB. If there are any outlier reference stars (stars that didn’t clear the NEB check) in the dmagRMS-plot (*Figure 2*) they must be removed and selected as target stars. Deselecting the defective reference stars makes them target stars which affects the light curve notably because the depth of those stars as a comparison star was affecting the T1 irregularly (3).

3.6 Generating a Light Curve

In section 3.4 when AstroImageJ generated a measurement table it also generated a light curve. However, to view our data on the light curve we have to format and adjust certain parameters. There are three different windows in AstroImageJ used to format and fit the light curve. In the “Multi-plot Main” section we changed the default X-data to be BJD_TBD and set the V. Marker 1 to our ingress time (0.713) and V. Marker 2 to our egress time (0.754). In the “Fit and Normalize Region Selection” window we set the orbital period of T1 to be 1.62 days and $R^*(R_{\text{sun}})$ to be 1.1 (15). The stellar radius of our host star is not available so we set it default to 1.1 times the radius of the Sun. There are also no Linear LD u1 and Quad LD u2 (limb darkening coefficients) for any TESS object of interest so we set both of them default to 0.3. However, since we unlocked Linear LD u1, the value of it changed to 0.199. To make sure there were no flawed reference stars corrupting the light flux of T1 we reviewed each reference star on the light curve and deselected any reference star that had big spreads in their flux. The reference stars near the perimeter of our field view had the biggest spreads and since they were deselected as reference stars, they became target stars (*Figure 1*).

To plot our data we used the “Multi-plot Y-data” tool to select the datasets that will be on the light curve. We compiled 10 plots that were stacked on top of each other. When we performed multi-aperture photometry the flux for our target and reference stars were recorded with a corresponding time in BJD_TBD. The normalized flux of T1 is the raw brightness flux data plotted without any detrending, however, this flux does not fit the transit model without detrending because there are systematic trends and external factors that cause the data to be diluted. To fix this we used the “Fit and Normalize

Region Selection" tool to test different detrend parameters that would yield the lowest BIC (Bayesian Information Criterion) and RMS (Root Mean Square) value. A lower BIC and RMS value would imply that the data is better fitted to the transit model. The two deterred parameters we used was AIRMASS and the flux of one the reference stars. AIRMASS is generally a good deterred parameter because it takes into account how much atmosphere our telescope looks through before we observe our

3.7 Probabilistic Transit Modeling

To determine the planetary radius of TOI 3779.01 we used the exoplanet python package to perform probabilistic transit modeling. The first transit model we generated was not a probabilistic plot but a normalized flux vs time plot of our target host star using PyMC3 (*Figure 3*). This is the exact same normalized flux plot of T1 created in AstroImageJ in section 3.6. To perform Bayesian probabilistic modeling to find the planet radius, we first initialized certain parameters with our prior belief of the value which we obtained from the transit model parameters in AstroImageJ. We set the baseline flux of our target host star to $0.065375461 \pm 0.013075092$, time of the reference transit (t_0) to 2459989.7337 ± 0.015 (BJD_TBD), orbital period to 1.618 days, and limb darkening parameters to 0.3 for both u_1 and u_2 . The impact parameter (b) is also initialized which is another variable which calculates the distance from the center of the host star to the center of the target exoplanet (Nighswander, 2017). The final parameter needed for the modeling is the planet-to-star radius ratio (r). However, since we did not have the r value, we set bounds for the r distribution with the lower bound as 0.01 and upper bound as 0.1.

A Markov chain is a process that utilizes the Markov property to determine possible outcomes where the probability of transitioning from one state to another is not dependent on the previous state or the path it took to get to the current state (17). MCMC is a set of algorithms that creates a Markov chain with a random distribution which eventually converges to the target posterior distribution (stationary distribution) (17). We then generated samples for each of these variables from the posterior distribution which is necessary to estimate the value of the planet-to-star radius ratio (r). The posterior distribution is the updated estimates and projections of the parameters after obtaining new data and information (18). For our samples to be accurate and reliable the MCMC chains must converge. So we ran a convergence test

target. We also plotted the residuals of T1 which had error bars of each data point to show the uncertainty and accuracy of the points in comparison to the transit model. Below the residuals we plotted the flux graphs of the two closest reference stars detrended with AIRMASS. Finally, at the bottom of our light curve we included 5 plots which were some of the available detrending parameters: WIDTH_T1, AIRMASS, tot_C_cnts, X(FITS)_T1, and Y(FITS)_T.

for each of our parameters (period, t_0 , r , b , u , mean) and the result is a table that summarizes the updated estimates of our parameters (Table 2). To visualize the posterior distribution of our radius and period we generated a corner plot (*Figure 5*). The corner plot and table generated from the posterior distribution after sampling can be used to determine the value of the planet-to-star radius ratio (r). In section 6 we will discuss how to use the planet-to-star radius ratio (r) and transit depth to find the planet radius of TOI 3779.01

4. Results

In this section we present the results of the light curve transit modeling and probabilistic modeling outlined in section 3. Our first output is a plot with the raw brightness flux of TOI 3779.01 over time (BJD_TBD) without any detrending (*Figure 3*). There is no apparent transit in this model due to the many external factors that cause the data to be defective. So we generated a new light curve in AstroImageJ that is detrended using the AIRMASS parameter and the flux of C5 a reference star (*Figure 4*). Detrending the normalized flux of T1 yielded a flux plot that follows the transit model close to the predicted ingress and egress times with a transit depth of 6.93 ppt. The light curve model clearly shows the dimming of the host star during the transit period. After completing the NEB analysis, reference stars C6 with a transit depth of 8.0 ppt and C24 with a transit depth of 11.3 did not clear the NEB check so we deselected them as reference stars. In section 3.6 we also deselected C5, C9, C10, C11, C12, and C13 due to their large spreads in flux. To determine the planet radius of TOI 3779.01 we generated a corner plot (*Figure 5*). The r parameter (planet-to-star radius ratio) in the corner plot has the highest concentration when r is estimated to be 0.037 ± 0.001 (Table 2). In section 5 we will discuss how to use the transit depth calculated from the AstroImageJ transit model (6.93 ppt) to derive the planet radius of TOI 3779.01.

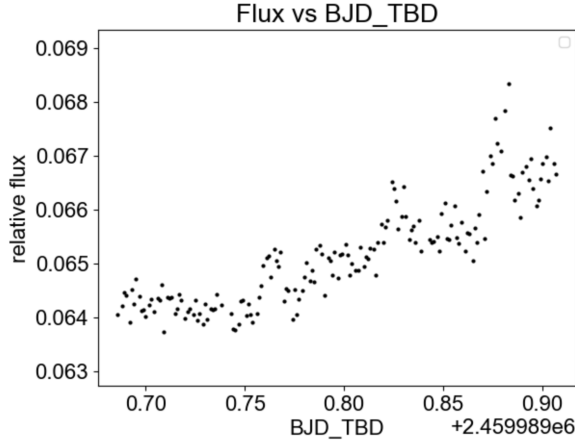


Figure 3 Flux graph vs BJD with no detrending

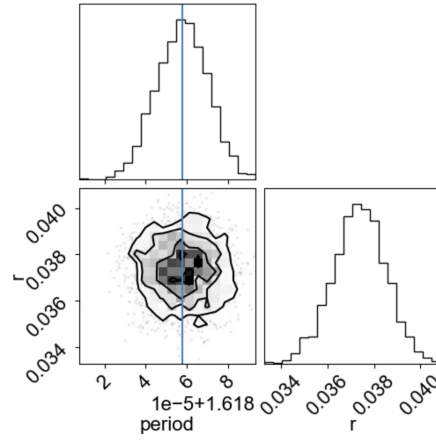


Figure 5 Corner Plot displaying the distributions of “period and “r”

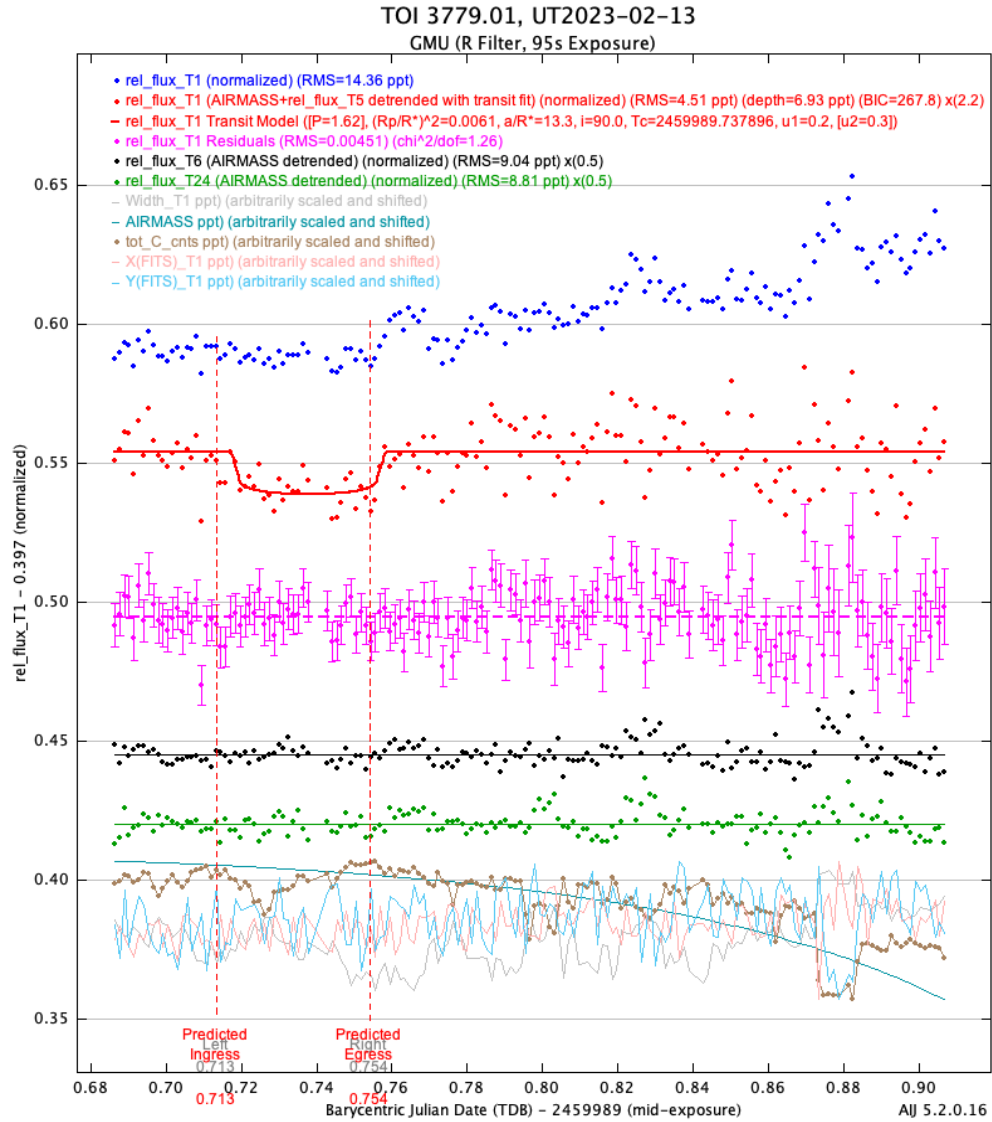


Figure 4 Light Curve generated through AstroImageJ. The red plot models a full transit of TOI 3779.01.

	mean	sd	hdi_3%	hdi_97%
period	1.618	0.000	1.618	1.618
t0	2459989.732	0.001	2459989.730	2459989.735
r	0.037	0.001	0.035	0.039
b	0.053	0.038	0.000	0.122
u[0]	0.350	0.209	0.000	0.708
u[1]	-0.050	0.175	-0.371	0.276
mean	0.066	0.000	0.066	0.066

	mcse_mean	mcse_sd	ess_bulk	ess_tail	r_hat
period	0.000	0.000	1631.0	1314.0	1.0
t0	0.000	0.000	1287.0	921.0	1.0
r	0.000	0.000	1947.0	1552.0	1.0
b	0.001	0.001	1995.0	991.0	1.0
u[0]	0.005	0.004	1448.0	938.0	1.0
u[1]	0.004	0.003	1682.0	1516.0	1.0
mean	0.000	0.000	1650.0	1204.0	1.0

Table 2 Summary table generated from the posterior distribution

5. Discussion

To classify TOI 3779.01 we need to examine our results and do statistical analysis to validate if it is an exoplanet. The light curve generated through AstroImageJ had a clear transit in the predicted time frame (*Figure 4*). With the two detrending parameters outlined in section 3.6 the flux data fitted much better to the model reducing the BIC (Bayesian Information Criterion) and RMS (Root Mean Square) significantly to 267.757 (BIC) and 4.508 (RMS). For our data to fit well to the target transit model it must also have a chi-square per degrees of freedom value close to or equal to 1.

$$\chi^2_v = \frac{\chi^2}{V}$$

Equation 1 Where χ^2 is chi-square and V is dof (19)

Using our chi-square value of 199.782 and dof value of 159 in Equation 1, our chi-square per degrees of freedom value is 1.256 which is close to 1. This means that the flux we observed of TOI 3779.01 is really close to the desired values. Based on the light curve alone it seems that TOI 3779.01 is an exoplanet upon observing a full transit, however, to classify it we need to determine its radius. In section 4 we estimated the planet-to-star radius ratio using probabilistic modeling to be 0.037 ± 0.001 . This value is a prediction from a posterior distribution which had converged from a random distribution. This is consistent and close to the radius value derived from the transit depth predicted from TESS (8.8 ppt). For any exoplanet a very accurate approximation for the transit depth is the ratio of the radius of the planet and radius of the host star squared (20).

$$\Delta F = \frac{F_{no\ transit} - F_{transit}}{F_{transit}} = \left(\frac{R_p}{R_\odot}\right)^2$$

Equation 2 Where F is the flux, R_p is the planet radius, and R_\odot is the stellar radius (21)

Since we don't have the radius of our host star we assumed that the stellar radius to be 1.1 times the radius of the sun. Using the transit depth calculated in AstroImageJ of our model (6.93 ppt) and *Equation 2* we determined the planet radius of TOI 3779.01 to be $0.09152 R_\odot$. This value is really close to $0.103189 R_\odot$ which is the planet radius calculated using the predicted transit depth from TESS (8.8) and *Equation 2*. Our derived radius also aligns with the R_{Jup} (Jupiter Radius or Jovian Radius) value calculated from the transit model in AstroImageJ which was 0.84. This means that our exoplanet is about 84 percent the size of Jupiter. Since the planet radius we calculated is really close to a Jupiter sized planet, we classified our exoplanet as a **Hot Jupiter**.

There are two main ways in which a Hot Jupiter can form. A Hot Jupiter can either form by core accretion (core contraction due to gravity) or gravitational instability (22). Core accretion causes a small proto-planet to amass a lot of gas and dust particles from the planetary disk around the proto-planet (22). Gravitational instability is when clumps of gas from the planetary disk get pulled into the planet due to gravitational forces adding to mass and size of the planet (22). Both Core accretion and gravitational instability cannot occur near a star due to the gas conditions near a star so Hot Jupiters are formed much farther away (22). However, when the orbit of Hot Jupiters becomes very elliptical they go through a process called Tidal migration where the orbit gradually becomes circular due to gravitational forces from the host star (22).

6. Conclusions

In our study we were able to successfully generate light curves and do probabilistic modeling. However, light curves and modeling are just the first steps in validating an exoplanet. To validate if TOI 3779.01 is a Hot Jupiter and not an NEB due to aperture contamination, this target can be researched by other TFOP sub-groups to perform more detailed

false-positive validation analysis like radial velocity measurements and spectroscopy. High contrast imaging can also be used to identify nearby faint stars which can also contaminate the aperture.

Acknowledgments

We want to thank Ian Helm for collecting the telescope data from GMU Observatory. This study wouldn't have been possible without the data he recorded. We also give special thanks to the Department of Physics and Astronomy at George Mason University for guiding us and providing the resources and tools needed for this research.

References

1. NASA. (2015, December 17). Exoplanet exploration: Planets beyond our solar system. <https://exoplanets.nasa.gov/>
2. Guerrero, N. (2023, April 20). TESS Transiting Exoplanet Survey Satellite. <https://tess.mit.edu/>
3. Conti, D. M. (2020, September 4). *TFOP SGI observation guidelines revision 6.4*. TFOP_SG1_Guidelines_Latest. https://astrodennis.com/TFOP_SG1_Guidelines_Latest.pdf
4. Rodriguez, J. E. (2023, April 20). Another Shipment of Six Short-Period Giant Planets from TESS. <https://arxiv.org/pdf/2205.05709.pdf>
5. Tang, S., & Waalkes, W. (2020, January). Ground-based follow-up observations of TESS Exoplanet Candidates. *Journal of Emerging Investigators*. <https://emerginginvestigators.org/articles/ground-based-follow-up-observations-of-tess-exoplanet-candidates/pdf>
6. TESS Project Candidates. NASA Exoplanet Archive. (2021, June 23). <https://exoplanetarchive.ipac.caltech.edu/cgi-bin/TblView/nph-tblView?app=ExoTbls&config=TOI>
7. Astronomy at Swarthmore College. (n.d.). Transit Finder. <https://astro.swarthmore.edu/transits/>
8. Plavchan, P., Matzko, W., Hamze, B., Wittrock, J., Bowen, M., Alfaro, O., & Collins, K. (n.d.). *Campus telescope tess follow-up light curve tutorial - schar program*. Google Docs. https://docs.google.com/document/d/1MZU2kb9ahNhv7tdghKX7EUUo-ub_7mJr/edit
9. Mackey, D. F. (2018). exoplanet. exoplanet docs. <https://docs.exoplanet.codes/en/latest/>
10. AstroImageJ 2.4.1 User Guide plus Getting Started with Differential Photometry. (n.d.). https://www.astro.louisville.edu/software/astroimagej/guide/AstroImageJ_User_Guide.pdf
11. *Batman: Bad-ass transit model calculation*. batman: Bad-Ass Transit Model cAlculation N - batman 2.4.6 documentation. (n.d.). <https://lkreidberg.github.io/batman/docs/html/index.html#>
12. Richmond, M. (n.d.). Simple Aperture Photometry by Hand. <http://spiff.rit.edu/classes/phys445/lectures/photom/photom.html#:~:text=Aperture%20photometry%20is%20the%20measurement,pressing%20the%20%22a%22%20key>
13. Astronomy at Swarthmore College. (n.d.). Annotated finding charts. https://astro.swarthmore.edu/transits/finding_charts.cgi
14. Harvard CFA. (n.d.). Sensing the Dynamic Universe: Eclipsing Binaries. <https://lweb.cfa.harvard.edu/sdu/eclipsingbinaries.html>
15. *Exofop TIC 742648307*. ExoFOP. <https://exofop.ipac.caltech.edu/tess/target.php?id=742648307>
16. Nighswander, M. (2017, January 25). The Exoplanet Transit Method. PaulAnthonyWilson.com | Observational Astronomer. <https://www.paulanthonywilson.com/exoplanets/exoplanet-detection-techniques/the-exoplanet-transit-method/>
17. Agrahari, S. (2021, July 30). Monte Carlo Markov Chain (MCMC) explained. Medium. <https://towardsdatascience.com/monte-carlo-markov-chain-mcmc-explained-94e3a6c8de11>
18. Stephanie. (2023, February 24). Posterior probability & the posterior distribution. Statistics How To. <https://www.statisticshowto.com/posterior-distribution-probability/>
19. Zarbock, R. (n.d.). Chi Squared per Degrees of Freedom. The Cosmic Effect. <https://sites.google.com/view/the-cosmic-connection/home/chi-squared-per-degrees-of-freedom>
20. Heller, R. (2019, March 20). Analytic solutions to the maximum and average exoplanet transit depth for common stellar limb darkening laws. *Astronomy & Astrophysics*. https://www.aanda.org/articles/aa/full_html/2019/03/aa34620-18/aa34620-18.html
21. Afanasev, D. (n.d.). Detection of exoplanets using the transit method - arxiv.org. <https://arxiv.org/pdf/1803.05565>
22. Fortney, J. J. (2021, February 8). Hot Jupiters: Origins, Structure, Atmospheres - Wiley Online Library. *Advancing Earth and Space Sciences*. <https://agupubs.onlinelibrary.wiley.com/doi/10.1029/2020JE006629>